HHS Public Access

Author manuscript

DNA Repair (Amst). Author manuscript; available in PMC 2021 March 23.

Published in final edited form as:

DNA Repair (Amst). 2018 December ; 72: 10–17. doi:10.1016/j.dnarep.2018.10.001.

Inactive Atm abrogates DSB repair in mouse cerebellum more than does Atm loss, without causing a neurological phenotype

Efrat Tal[a], **Marina Alfo**[a], **Shan Zha**[b], **Ari Barzilai**[c], **Chris I. De Zeeuw**[d], **Yael Ziv**[a], **Yosef Shiloh**[a,*]

[a]The David and Inez Myers Laboratory for Cancer Research, Department of Human Molecular Genetics and Biochemistry, Sackler School of Medicine, New York, United States [b]Institute for Cancer Genetics, Department of Pathology and Cell Biology, College of Physicians and Surgeons, Columbia University, New York, NY, United States [c]Department of Neurobiology, George S. Wise Faculty of Life Sciences, and Sagol School of Neuroscience, Tel Aviv University, Tel Aviv, Israel [d]Department of Neuroscience, Erasmus Medical Center, Rotterdam, and the Royal Netherlands Academy of Art & Science, Amsterdam, Netherlands

Abstract

The genome instability syndrome, ataxia-telangiectasia (A-T) is caused by null mutations in the *ATM* gene, that lead to complete loss or inactivation of the gene's product, the ATM protein kinase. ATM is the primary mobilizer of the cellular response to DNA double-strand breaks (DSBs) – a broad signaling network in which many components are ATM targets. The major clinical feature of A-T is cerebellar atrophy, characterized by relentless loss of Purkinje and granule cells. In *Atm*-knockout (*Atm*-KO) mice, complete loss of Atm leads to a very mild neurological phenotype, suggesting that Atm loss is not sufficient to markedly abrogate cerebellar structure and function in this organism. Expression of inactive ("kinase-dead") Atm (Atm^{KD}) in mice leads to embryonic lethality, raising the question of whether conditional expression of Atm^{KD} in the murine nervous system would lead to a more pronounced neurological phenotype than Atm loss. We generated two mouse strains in which Atm^{KD} was conditionally expressed as the sole Atm species: one in the CNS and one specifically in Purkinje cells. Focusing our analysis on Purkinje cells, the dynamics of DSB readouts indicated that DSB repair was delayed longer in the presence of Atm^{KD} compared to Atm loss. However, both strains exhibited normal life span and displayed no gross cerebellar histological abnormalities or significant neurological phenotype. We conclude that the presence of Atm^{KD} is indeed more harmful to DSB repair than Atm loss, but the murine central nervous system can reasonably tolerate the extent of this DSB repair impairment. Greater pressure needs to be exerted on genome stability to obtain a mouse model that recapitulates the severe A-T neurological phenotype.

*Corresponding author. yossih@post.tau.ac.il (Y. Shiloh).

Conflicts of interest The authors declare that there are no conflicts of interest.

Keywords

Ataxia-telangiectasia; ATM; Kinase-dead; DNA damage response; Double-strand breaks; Cerebellar atrophy

1. Introduction

The DNA damage response (DDR) is a main axis of genome stability [1,2]. Severe DDR defects lead to genome instability syndromes, which usually combine tissue degeneration, cancer predisposition, segmental premature aging, and sensitivity to DNA damaging agents [3–7]. The corresponding mouse models are important for understanding the link between impaired DDR and the resultant phenotypes [8,1–10].

A prototype genome instability disorder is ataxia-telangiectasia (A-T), a highly pleiotropic, autosomal recessive human disorder [11] caused by mutations in the *ATM* (A-T, mutated) gene [12,13], which encodes the ATM protein [14,15]. ATM is a homeostatic protein kinase with many physiological functions [15,16–22]. A widely documented one is its role as the chief mobilizer of the cellular response to DNA double-strand breaks (DSBs), a complex, tightly regulated signaling network that modulates numerous branches of cellular physiology in response to DSB induction [2,15,23,24]. ATM activates and regulates this network by phosphorylating a multitude of substrates in its various branches [15,17,18,25,26]. ATM belongs to a family of PI-3 kinase-like protein kinases (PIKKs), which includes, among others, the catalytic subunit of the DNA-dependent protein kinase (DNA-PKcs) and ATR, both of which are also involved in responding to genotoxic and other stresses [27].

Most A-T mutations are null alleles that truncate the ATM protein. Since truncated ATM is usually unstable, most A-T patients are typically devoid of ATM [11,28]. The prominent symptom is progressive cerebellar ataxia that develops into severe motor dysfunction [11,29]. The main underlying pathology is progressive cerebellar degeneration that involves primarily Purkinje cells (PCs) and granule neurons. Peripheral neuropathy may develop during the second decade of life. Oculocutaneous telangiectasia (dilated blood vessels) appear variably in the eyes and facial skin. Marked immunodeficiency is manifested by reduction of various immunoglobulin isotypes, and diminished B and T lymphocyte counts. Lung infections often result from food aspiration combined with the immunodeficiency. Another hallmark is gonadal and thymic dysgenesis. Cancer predisposition is manifested as increased tendency to develop lymphoreticular malignancies, and various carcinomas appear in older patients. Growth retardation and occasional endocrine abnormalities are also seen, among them insulin-resistant diabetes. An important, emerging aspect of A-T is premature aging [17],'evidenced in part by the markedly accelerated senescence found in primary fibroblasts derived from A-T patients [30]. Major laboratory findings are elevated serum levels of alpha-fetoprotein and carcinoembryonic antigen. A-T patients show a striking sensitivity to the cytotoxic effect of ionizing radiation (IR), and cultured A-T cells exhibit marked chromosomal instability, sensitivity to IR and radiomimetic chemicals, and reduced telomere length. IR sensitivity results from a profound defect in initiating the ATM-dependent response to DSBs.

Many A-T symptoms can be attributed to the abrogation of the cellular response to DSBs, both physiological ones and those induced by endogenous reactive oxygen species. However, the cause of the most devastating symptom – the progressive cerebellar atrophy – is still being debated, in view of the many physiological functions of ATM in addition to its role in the DSB response [15–17,19–22,31–50]. An important research tool in the attempts to understand this component of the A-T phenotype is mouse models of A-T.

Most mouse models of A-T are based on truncating or frameshift mutations in the murine *Atm* gene, similar to the null *ATM* mutations that cause A-T in humans. Atm-deficient mice were found to recapitulate major A-T symptoms, including the profound cancer predisposition, acute radiation sensitivity and sterility, but were largely spared the progressive cerebellar atrophy [51–54]. Several studies noted, however, morphological and functional abnormalities in the cerebellar cortex of Atm-deficient mice, such as ectopic and abnormally differentiated Purkinje cells [54], decreased duration of calcium currents and firing in these cells [55], and degenerative changes in several types of neurons, identified using electron microscopy [56]. Further abnormalities were observed in tissue organization and various physiological and molecular circuits of the murine Atm-deficient nervous system [39,51–70]. It appears, therefore, that Atm loss in the mouse can cause physiological damage in various tissues, similar to what is seen in A-T patients, but unlike the human cerebellum, the murine cerebellum can largely tolerate Atm loss and maintain its neuromotor functions. Furthermore, daily monitoring of Atm-deficient mice in our colonies turned up no behavioral abnormalities in animals up to 2 years of age. One possible approach to obtaining a mouse model of A-T that will exhibit cerebellar atrophy is to induce Atm mutations in this organism that will produce a harsher effect than that caused by the null alleles that eliminate the Atm protein. Such are mutations that produce catalytically inactive (‘kinase-dead’) Atm.

Yamamoto et al. [71] and Daniel et al. [72] showed that expression of physiological levels of kinase-dead in mice Atm leads to early embryonic lethality. Furthermore, cultured cells expressing inactive Atm exhibited greater genome instability compared to Atm-deficient cells [71,72]. Detailed mechanistic explanations for this observation are lacking, but it is assumed that the presence of inactive Atm interferes with the cellular response to genotoxic stress, such as the cleavage of trapped protein adducts in replicating cells [73], and perhaps other ATM-dependent pathways more than does the absence of Atm [74]. We asked therefore whether conditional expression of kinase-dead Atm in the nervous system of the mouse will exert a more profound cerebellar effect than Atm loss.

2. Materials and methods

2.1. Mouse strains

Animals were held in a specific pathogen-free facility. All experimental procedures complied with the standards as defined by the National Institutes of Health Guide for the Care and Use of Laboratory Animals and approved by the Tel Aviv University Institutional Animal Care and Use Committee.

The study was carried out using mice with a mixed C57BL/129 Sv background. The following *Atm* alleles were used: an *Atm*-knockout allele (Atm^{-}) [51] (B6.129S6-Atm^{tm1Awb}/J in the Jackson Labs Repository); a 'floxed' *Atm* allele (Atm^{fl}) containing loxP sites flanking exons 57–58 of the gene [75,76] (strain 129-$Atm^{tm2.1Fwa}$/J in Jackson Labs; and a kinase-dead *Atm* allele (Atm^{KD}), which produces an Atm protein with two inactivating amino acid substitutions (D2880 A/N2885 K) in its catalytic domain [71]. Cre recombinase expressed from a transgene driven by the Nestin promoter (strain B6.Cg-Tg(Nes-cre) 1Kln/J in the JAX Repository) was used to inactivate floxed alleles in the central nervous systems [77]. The L7 (Pcp2) promoter was used to express Cre in PCs [78] (JAX strain Tg(Pcp2-cre)1Amc/J).

2.2. Antibodies

The following antibodies were used: polyclonal goat anti-Calbindin D28 K (Santa Cruz Biotechnology Inc., Santa Cruz, CA), monoclonal mouse anti-Neuronal Nuclei (NeuN) (Millipore, Billerica, MA), polyclonal rabbit anti GABA(A) receptor alpha 6 subunit receptor (Millipore, Temecula, CA), monoclonal mouse anti-pS139-H2AX (Merck Millipore, Darmstadt, Germany), polyclonal rabbit anti-53BP1 (Novus Biologicals, Littleton CO), monoclonal rabbit anti-ATM D2E2 (Cell Signaling, Danvers, MA), polyclonal rabbit anti-pS824-KAP-1 (Bethyl Laboratories, Montgomery, TX), monoclonal mouse anti-KAP-1 (BD Transduction Laboratories, San Jose, CA), monoclonal mouse anti-HSC70 (Santa Cruz Biotechnology Inc., Santa Cruz, CA).

2.3. Inhibitors

DNA-PK inhibitor: NU7441 (Tocris Bioscience, Bristol, UK). ATR inhibitor: AZ20 (Tocris).

2.4. X-irradiation

Mice underwent total body irradiation using an X-irradiator (160 H F, Philips, Germany) at a dose rate of 1 Gy/min. Cultures were irradiated using an X-irradiator (Faxitron, Tucson, AZ) at a dose rate of 0.5 Gy/min.

2.5. Immunoblotting of mouse tissues

Irradiated mice were sacrificed 30 min after irradiation and organs were immediately harvested and snap-frozen in liquid nitrogen. Protein extraction and immunoblotting were performed as previously described [79,80].

2.6. Histological analysis

Mice were anesthetized with 1% Ketamine and 0.1% Xylazine solution (1 ml per 10 g of body weight) and sacrificed by PBS perfusion. Cerebellar tissues were fixed in 4% paraformaldehyde and dehydrated in graded ethanol series using the Leica TP1020 Tissue Processor. The tissues were cut into 10 μm parasagittal sections, deparaffinized in two 5 min incubations in xylene and rehydrated in a graded series of ethanol. The sections were then stained using hematoxylin and 1% eosin solution (Kaltec, Padova, Italy). For immunostaining, the sections were treated with antigen unmasking solutions (Vector Laboratories, Burlingame, CA), washed with PBS, and blocked with PBSTg (0.2% Tween,

0.2% gelatin in PBS). The tissue sections were then incubated with the primary antibody overnight, washed with PBS and PBSTg and incubated with the secondary antibody in PBS for 2 h. The sections were then washed and stained with 0.1 mg/ml 4,6-diamidino-2-phenylindole (DAPI), and mounted with aqueous mounting medium containing anti-fading agents (Biomeda Corp, Foster City, CA). Immunofluorescent images were captured using a Leica TCS SP2 confocal microscope (Leica Microsystems GmbH, Germany).

2.7. Cerebellar organotypic cultures

Cerebellar organotypic cultures were established and stained as previously described [81,82]. Cultures were X-irradiated 12 days after their establishment.

2.8. Behavioral analysis

Initial testing for possible behavioral changes reflecting cerebellar defects was based on the scoring scheme described by Guyenet et al. [83]. Mice were tested once every 1–3 months from 1 to 24 months of age. Tests included hind limb clasping, ledge test, gait and appearance of kyphosis [83]. Animals were also examined at 12 and 20 month using the computerized CatWalk gait analysis system (Noldus, Wagen-ingen, Netherlands, which recorded and subsequently analyzed the animals' footprints as they went along a glass runway 3 times. Mice were also tested for general locomotor activity and willingness to explore using an open field test performed in a 50 × 50 cm arena for 20 min. Their motion was recorded using a GigE color 1/2″ Basler acA1300–60gc camera (Basler, Ahrensburg, Germany) and analyzed using EthoVision XT 11.5 software (Noldus). The CatWalk and Open Field tests were carried out in the Myers Neuro-Behavioral Core Facility of Tel Aviv University.

3. Results

3.1. Generation of mice expressing no Atm or kinase-dead Atm in the CNS or in PCs only

Mice in which *Atm* is conditionally ablated in the CNS (*Atm*-Δ-CNS) or specifically in PCs (*Atm*-Δ-PC) were obtained by combining an $Atm^{-/fl}$ genotype with expression of Nes-Cre or Pcp2-Cre, respectively. (The use of a floxed *Atm* allele against a null allele was intended to increase the chance of eliminating the Atm protein in the target cells by reducing the occurrence of excision of one out of two floxed alleles). Lifespan and cage behavior of both the *Atm*-Δ-CNS and *Atm*-Δ-PC animals were normal. Mice expressing Atm^{KD} in the CNS or specifically in PCs (*Atm*-KD-CNS and *Atm*-KD-PC, respectively) were obtained by combining the Nes-Cre or Pcp2-Cre transgenes with an $Atm^{fl/KD}$ genotype (Fig. 1). In these animals, the Atm^{fl} allele was expected to be inactivated by the Cre recombinase, leaving Atm^{KD} as the only viable *Atm* allele in Creexpressing cell types. Of note, the $Atm^{fl/KD}$ genotype itself (which is common to all body cells) does not cause any discernible phenotype [71]. Both the *Atm*-KD-CNS and *Atm*-KD-PC mice were viable and completed a normal lifespan. Notably, the body weight of the mice expressing the Nestin-Cre was reduced compered to non-Nestin-Cre expressing animals (Supplementary Fig. 1). This was previously reported and attributed to metabolic effects of nestin promoter-driven expression of the Cre recombinase [84].

3.2. Atm level and activity readout in tissues of mice with different Atm genotypes

Immunoblotting analysis of tissue extracts from the *Atm*-Δ-CNS mice indicated that Atm protein level was below detection in the cerebrum and cerebellum of these animals (Fig. 2a). As expected, the Atm signal obtained from CNS tissues of the *Atm*-KD-CNS animals was lower than that of WT tissues (Fig. 2a), since it represented only one allele that expresses the mutant protein. We also examined a well-documented readout of ATM activity after DSB induction: the robust phosphorylation of its substrate, KAP-1 on Ser824, which is detected using a highly specific anti-phospho antibody [85]. Indeed, 30 min following treatment of the animals with 10 Gy of IR, Kap-1 phosphorylation in the *Atm*-Δ-CNS and *Atm*-KD-CNS animals was considerably reduced in the CNS but not in the spleen, which served as the control tissue (Fig. 2a). This result indicated that Atm^{KD} was indeed catalytically inactive in the *Atm*-KD-CNS animals. The residual phosphorylation of Kap-1 that is occasionally detected in the absence of Atm activity in the brain (Fig. 2a) is attributed primarily to DNA-PK [76] (and our unpublished data). Similar results were obtained in cerebellar organotypic (slice) cultures, which we routinely use to analyze the cerebellar DDR [81,82]. These cultures maintain the organization of the cerebellar tissue for several weeks in culture and are amenable to treatment with DNA damaging agents [65,81,82]. The cultures were irradiated, and phosphorylations of histone H2ax and Kap-1 were detected using immunostaining. Both phosphorylations were profoundly down-regulated in *Atm*-Δ-CNS and *Atm*-KD-CNS cultures (Fig. 2b). Notably, this result suggests that in this tissue Atm has a major role in H2ax and Kap1 phosphorylation in response to DSB induction. Importantly, a small, distinct group of cells exhibited vigorous Kap-1 phosphorylation in both mutant genotypes (Fig. 2b), presumably representing cells in which the Nestin promoter had not been activated during development or cells in which the floxed Atm allele had escaped Cre-mediated excision.

We used inhibitors against DNA-PK and ATR to assess the share of each of the three PIKKs in these phosphorylations in the murine cerebellum. Inhibition of Dna-pk or Atr in Atm-proficient, $Atm^{f/f}$ cells reduced the two phosphorylations considerably (Fig. 2b), pointing to the importance of concerted action of these kinases in these damage-induced phosphorylations in this organ.

Fig. 2c presents similar analysis of cerebellar organotypic cultures derived from *Atm*-Δ-PC and *Atm*-KD-PC mice demonstrating the lack of Atm activity specifically in PCs of both genotypes.

3.3. Expression of catalytically inactive Atm in the CNS impairs DSB repair in PCs, more than Atm absence

In order to follow DSB repair in PCs with the various *Atm* genotypes, we used cerebellar organotypic cultures treated with IR. We monitored in PCs the dynamics of two immunofluorescent DSB readouts: nuclear foci of phosphorylated histone H2ax (γH2ax) and the DDR protein, 53bp1 [86]. In the early time points after irradiation, the response in Atm-deficient cells was reduced compared to Atm-proficient cells, but later on, the decline in foci number over time, which is considered to represent DSB repair, was delayed in PCs from *Atm*-Δ-CNS and *Atm*-KD-CNS animals compared to the $Atm^{fl/fl}$ genotype (Fig. 3c, d).

Importantly, the delay in DSB repair was greater in PCs in *Atm*-KD-CNS cultures than in those of *Atm*-Δ-CNS mice (Fig. 3c, d). This result suggests that the presence of kinase-dead Atm in the CNS exerts a more pronounced effect on DSB repair than Atm absence. This result is in accord with previous findings showing greater genome instability in murine embryonic stem cells and lymphocytes expressing kinase-dead Atm compared to those lacking Atm altogether [71,72]. Interestingly, however, when Atm loss or replacement by a kinase-dead protein was confined to PCs, the increased impact on DSB repair of inactive Atm compared to Atm loss was not observed (Fig. 3e, f). It should be stressed in this regard that, in the *Atm*-KD-PC expression of kinase-dead Atm was confined to PCs while the surrounding cells contained normal levels of WT Atm, as evidenced by the Atm activity assay (Fig. 2c).

3.4. Conditional expression of inactive atm in the CNS or just in PCs does not lead to a significant neurological phenotype

The animals expressing kinase-dead Atm in the CNS or in PCs were tested every 1–3 months from 1 to 24 months using the Gait Test and Ledge Test that measure coordination of movements, and the Hind Limb Clasping Test, that can highlights severe cerebellar abnormalities. Special attention was paid to the appearance of kyphosis, which may be caused by the loss of muscle tone in the spinal muscles secondary to neurodegeneration [83]. No abnormalities were observed in these parameters in the two mutant genotypes (data not shown) during the 24 months. When the mice were evaluated at 20 months using the Open Field and CatWalk systems *Atm*-KD-CNS, but not *Atm*-KD-PC mice demonstrated changes in their footprints suggesting alterations in stepping pattern and coordination (Fig. 4e). However, collectively all other parameters did not detect behavioral pattern suggesting cerebellar dysfunction (Fig. 4). Similar to the normal neurological phenotype observed in mice expressing kinase-dead Atm in the CNS, *Atm*-Δ-CNS mice expressing no Atm protein in the CNS also displayed no significant phenotype. Some behavioral changes were observed in the *Atm*-Δ-CNS and Nestin-Cre-expressing mice which might due to the Cre expression in the tissue (Supplementary Fig. 2). We concluded that conditional expression of Atm^{KD} in the CNS or PCs did not lead to changes in behavior indicative of motor deficits.

The cerebellar structure and organization of the animal were examined every 3 months from 3 weeks to 24 months using hematoxylin-eosin staining and immunohistochemical staining of cell type markers. No gross organizational abnormalities in the cerebella of the *Atm*-KD-CNS and *Atm*-KD-PC animals were observed during this period (Fig. 5).

4. Discussion and conclusions

The conditional ablation of the *Atm* gene in the *Atm*-Δ-CNS mouse allows circumventing the extreme cancer predisposition of the $Atm^{-/-}$ genotype leading to Atm loss in all body tissues, and enables following the animal's neuromotor performance throughout a full life span. Expression of Atm^{KD} in the CNS was expected to take the pressure on genome stability one step further. Our and previous [71,72] results suggest that conditional expression of Atm^{KD} in various tissues does not lead to the embryonic lethality caused by whole body expression of inactive Atm. The embryonic lethality may result from

interference with a critical developmental step. However, if that step is successfully executed, the DDR abrogation caused by Atm^{KD} expressed conditionally in a specific tissue is not sufficient to undermine the tissue's integrity or function. Thus, intensifying the DSB repair defect associated with Atm loss by expressing Atm^{KD} in the murine CNS was not sufficient to affect the structure and function of the corresponding cell types and the tissue at large. The practical conclusion from these results is that, in order to obtain a mouse model that satisfactorily recapitulates the A–T neurological phenotype, further abrogation of the DNA damage response or exertion of higher genotoxic pressure on the murine cerebellum might be required.

It is still interesting, why Atm^{KD} exerts a more pronounced effect on DSB repair compared to Atm loss. A portion of nuclear ATM is recruited to DSB sites [87] and is thus part of the nuclear foci that are meticulously formed around these sites [88]. Many of the ATM-mediated phosphorylations occur within these protein structures, whose fine organization is critical for the delicate balance among DSB repair pathways and subsequently - timely DSB repair [89]. Importantly, Atm^{KD} is recruited to DSB sites same as active Atm [71,72]. The experimental results suggest that the presence of inactive Atm within the complex multiprotein structures that are constructed around DSBs abrogates their organization and subsequently DSB repair, more that ATM absence.

The comparison between *Atm*-KD-PC and *Atm*-KD-CNS animals highlighted a difference in the effect of Atm^{KD} on DSB repair in PCs surrounded by Atm^{KD}-expressing cells or PCs with Atm^{KD} surrounded by WT cells. This result may point to the importance of the surrounding cells in determining the functional outcome of PCs' own *Atm* genotype. Support for this concept comes from a recent study with mixed cell cultures, in which the functionality of Atm-deficient murine granule cells depended on the *Atm* genotype of astrocytes that interacted with them [90]. Thus, conditional expression of *Atm* genotypes in a specific cell type may yield different physiological results depending on the genotype of surrounding cells. Our results therefore surface certain limitations of the conclusions that can be drawn when the Cre-lox technology is used for tissue-specific gene manipulation. An overarching conclusion concerning A-T is emerging from studies based on CNS-specific ablation of the *Atm* gene in mice: the cerebellar atrophy in A-T may be influenced not only by Atm loss in specific cerebellar cell types, but also by lack of Atm in other tissues that neighbor or connect with the cerebellum.

Supplementary Material

Refer to Web version on PubMed Central for supplementary material.

Acknowledgments

We thank Ran Elkon for assistance with the statistical analyses and Julia Shaknof and Rotem Granit for technical assistance. Special thanks to Lior Bikovski for help with the behavioral tests carried out at the Myers Neuro-Behavioral Core Facility of Tel Aviv University. Work in the lab of Y.S. was supported by research grants from The A-T Children's Project, The Israel Ministry of Science and Technology, and the A-T Ease Foundation. Work in the lab of C.I.D.Z. was supported by the Dutch Organization for Medical Sciences, Life Sciences, ERC-adv and ERC-POC of the EU. Y.S. is a Research Professor of the Israel Cancer Research Fund.

References

[1]. Chatterjee N, Walker GC, Mechanisms of DNA damage, repair, and mutagenesis, Environ. Mol. Mutagen. (2017).

[2]. Goldstein M, Kastan MB, The DNA damage response: implications for tumor responses to radiation and chemotherapy, Annu. Rev. Med. 66 (2015) 129–143. [PubMed: 25423595]

[3]. O'Driscoll M, The pathological consequences of impaired genome integrity in humans; disorders of the DNA replication machinery, J. Pathol. 241 (2) (2017) 192–207. [PubMed: 27757957]

[4]. McKinnon PJ, Genome integrity and disease prevention in the nervous system, Genes Dev. 31 (12) (2017) 1180–1194. [PubMed: 28765160]

[5]. Ceccaldi R, Sarangi P, D'Andrea AD, The Fanconi anaemia pathway: new players and new functions, Nat. Rev. Mol. Cell Biol. 17 (6) (2016) 337–349. [PubMed: 27145721]

[6]. Liakos A, Lavigne MD, Fousteri M, Nucleotide excision repair: from neurodegeneration to cancer, Adv. Exp. Med. Biol. 1007 (2017) 17–39. [PubMed: 28840550]

[7]. Croteau DL, et al., Human RecQ helicases in DNA repair, recombination, and replication, Annu. Rev. Biochem. 83 (2014) 519–552. [PubMed: 24606147]

[8]. Lee K, Tosti E, Edelmann W, Mouse models of DNA mismatch repair in cancer research, DNA Repair (Amst) 38 (2016) 140–146. [PubMed: 26708047]

[9]. Vermeij WP, Hoeijmakers JH, Pothof J, Genome integrity in aging: human syndromes, mouse models, and therapeutic options, Annu. Rev. Pharmacol. Toxicol. 56 (2016) 427–445. [PubMed: 26514200]

[10]. Specks J, et al., Modeling the study of DNA damage responses in mice, Methods Mol. Biol. 1267 (2015) 413–437. [PubMed: 25636482]

[11]. Rothblum-Oviatt C, et al., Ataxia telangiectasia: a review, Orphanet. J. Rare Dis. 11 (1) (2016) 159. [PubMed: 27884168]

[12]. Savitsky K, et al., A single ataxia telangiectasia gene with a product similar to PI-3 kinase, Science 268 (5218) (1995) 1749–1753. [PubMed: 7792600]

[13]. Savitsky K, et al., The complete sequence of the coding region of the ATM gene reveals similarity to cell cycle regulators in different species, Hum. Mol. Genet. 4 (11) (1995) 2025–2032. [PubMed: 8589678]

[14]. Ziv Y, et al., Recombinant ATM protein complements the cellular A-T phenotype, Oncogene 15 (2) (1997) 159–167. [PubMed: 9244351]

[15]. Shiloh Y, Ziv Y, The ATM protein kinase: regulating the cellular response to genotoxic stress, and more, Nat. Rev. Mol. Cell Biol. 14 (4) (2013) 197–210.

[16]. Shiloh Y, ATM: expanding roles as a chief guardian of genome stability, Exp. Cell. Res. 329 (1) (2014) 154–161. [PubMed: 25218947]

[17]. Shiloh Y, Lederman HM, Ataxia-telangiectasia (A-T): an emerging dimension of premature ageing, Ageing Res. Rev. 33 (2017) 76–88. [PubMed: 27181190]

[18]. Paull TT, Mechanisms of ATM activation, Annu. Rev. Biochem. 84 (2015) 711–738. [PubMed: 25580527]

[19]. Guleria A, Chandna S, ATM kinase: much more than a DNA damage responsive protein, DNA Repair (Amst) (2015).

[20]. Choy KR, Watters DJ, Neurodegeneration in ataxia-telangiectasia: multiple roles of ATM kinase in cellular homeostasis, Dev. Dyn. 247 (1) (2018) 33–46. [PubMed: 28543935]

[21]. Zhang Y, et al., Mitochondrial redox sensing by the kinase ATM maintains cellular antioxidant capacity, Sci. Signal. 11 (538) (2018).

[22]. Lee JH, et al., ATM directs DNA damage responses and proteostasis via genetically separable pathways, Sci. Signal. 11 (512) (2018).

[23]. Sirbu BM, Cortez D, DNA damage response: three levels of DNA repair regulation, Cold Spring Harb. Perspect. Biol. 5 (8) (2013) p. a012724. [PubMed: 23813586]

[24]. Goodarzi AA, Jeggo PA, The repair and signaling responses to DNA double-strand breaks, Adv. Genet. 82 (2013) 1–45. [PubMed: 23721719]

[25]. Clouaire T, Marnef A, Legube G, Taming tricky DSBs: ATM on duty, DNA Repair (Amst) (2017).

[26]. Bensimon A, et al., ATM-dependent and -independent dynamics of the nuclear phosphoproteome after DNA damage, Sci. Signal. 3 (151) (2010) p. rs3.. [PubMed: 21139141]

[27]. Blackford AN, Jackson SP, ATM, ATR, and DNA-PK: the Trinity at the heart of the DNA damage response, Mol. Cell 66 (6) (2017) 801–817. [PubMed: 28622525]

[28]. Gilad S, et al., Predominance of null mutations in ataxia-telangiectasia, Hum. Mol. Genet. 5 (4) (1996) 433–439. [PubMed: 8845835]

[29]. Perlman SL, et al., Ataxia-telangiectasia, Handb. Clin. Neurol. 103 (2012) 307–332. [PubMed: 21827897]

[30]. Shiloh Y, Tabor E, Becker Y, Colony-forming ability of ataxia-telangiectasia skin fibroblasts is an indicator of their early senescence and increased demand for growth factors, Exp. Cell. Res. 140 (1) (1982) 191–199. [PubMed: 6213420]

[31]. Biton S, Barzilai A, Shiloh Y, The neurological phenotype of ataxia-telangiectasia: solving a persistent puzzle, DNA Repair (Amst) 7 (7) (2008) 1028–1038. [PubMed: 18456574]

[32]. Hoche F, et al., Neurodegeneration in ataxia telangiectasia: what is new? What is evident? Neuropediatrics 43 (3) (2012) 119–129. [PubMed: 22614068]

[33]. Yang Y, et al., The interaction of the atm genotype with inflammation and oxidative stress, PLoS One 9 (1) (2014) p. e85863. [PubMed: 24465754]

[34]. Ditch S, Paull TT, The ATM protein kinase and cellular redox signaling: beyond the DNA damage response, Trends Biochem. Sci. 37 (1) (2012) 15–22. [PubMed: 22079189]

[35]. McKinnon PJ, ATM and the molecular pathogenesis of ataxia telangiectasia, Annu. Rev. Pathol. 7 (2012) 303–321. [PubMed: 22035194]

[36]. Vail G, et al., ATM protein is located on presynaptic vesicles and its deficit leads to failures in synaptic plasticity, J. Neurophysiol. 116 (1) (2016) 201–209. [PubMed: 27075534]

[37]. Herrup K, ATM and the epigenetics of the neuronal genome, Mech. Ageing Dev. 134 (10) (2013) 434–439. [PubMed: 23707635]

[38]. Herrup K, Li J, Chen J, The role of ATM and DNA damage in neurons: upstream and downstream connections, DNA Repair (Amst) 12 (8) (2013) 600–604. [PubMed: 23680599]

[39]. Fang EF, et al., NAD+ replenishment improves lifespan and healthspan in ataxia telangiectasia models via mitophagy and DNA repair, Cell Metab. 24 (4) (2016) 566–581. [PubMed: 27732836]

[40]. Eaton JS, et al., Ataxia-telangiectasia mutated kinase regulates ribonucleotide reductase and mitochondrial homeostasis, J. Clin. Invest. 117 (9) (2007) 2723–2734. [PubMed: 17786248]

[41]. Li J, et al., EZH2-mediated H3K27 trimethylation mediates neurodegeneration in ataxia-telangiectasia, Nat. Neurosci. 16 (12) (2013) 1745–1753. [PubMed: 24162653]

[42]. Kim TS, et al., The ZFHX3 (ATBF1) transcription factor induces PDGFRB, which activates ATM in the cytoplasm to protect cerebellar neurons from oxidative stress, Dis. Model. Mech. 3 (11–12) (2010) 752–762. [PubMed: 20876357]

[43]. Yang DQ, et al., Cytoplasmic ATM protein kinase: an emerging therapeutic target for diabetes, cancer and neuronal degeneration, Drug Discov. Today 16 (7–8) (2011) 332–338. [PubMed: 21315178]

[44]. Ambrose M, Gatti RA, Pathogenesis of ataxia-telangiectasia: the next generation of ATM functions, Blood 121 (20) (2013) 4036–4045. [PubMed: 23440242]

[45]. Choy KR, Watters DJ, Neurodegeneration in ataxia-telangiectasia: multiple roles of ATM kinase in cellular homeostasis, Dev. Dyn. (2017).

[46]. Dahl ES, Aird KM, Ataxia-telangiectasia mutated modulation of carbon metabolism in cancer, Front. Oncol. 7 (2017) 291. [PubMed: 29238697]

[47]. Berger ND, et al., ATM-dependent pathways of chromatin remodelling and oxidative DNA damage responses, Philos. Trans. R. Soc. Lond. B Biol. Sci. 372 (1731) (2017).

[48]. Khoronenkova SV, Mechanisms of non-canonical activation of ataxia telangiectasia mutated, Biochemistry (Mosc). 81 (13) (2016) 1669–1675. [PubMed: 28260489]

[49]. Valentin-Vega YA, Kastan MB, A new role for ATM: regulating mitochondrial function and mitophagy, Autophagy 8 (5) (2012) 840–841. [PubMed: 22617444]

[50]. Fang EF, et al., NAD(+) replenishment improves lifespan and healthspan in ataxia telangiectasia models via mitophagy and DNA repair, Cell Metab. 24 (4) (2016) 566–581. [PubMed: 27732836]

[51]. Barlow C, et al., Atm-deficient mice: a paradigm of ataxia telangiectasia, Cell 86 (1) (1996) 159–171. [PubMed: 8689683]

[52]. Elson A, et al., Pleiotropic defects in ataxia-telangiectasia protein-deficient mice, Proc. Natl. Acad. Sci. U. S. A. 93 (23) (1996) 13084–13089. [PubMed: 8917548]

[53]. Xu Y, et al., Targeted disruption of ATM leads to growth retardation, chromosomal fragmentation during meiosis, immune defects, and thymic lymphoma, Genes Dev. 10 (19) (1996) 2411–2422. [PubMed: 8843194]

[54]. Borghesani PR, et al., Abnormal development of Purkinje cells and lymphocytes in Atm mutant mice, Proc. Natl. Acad. Sci. U. S. A. 97 (7) (2000) 3336–3341. [PubMed: 10716718]

[55]. Chiesa N, et al., Atm-deficient mice Purkinje cells show age-dependent defects in calcium spike bursts and calcium currents, Neuroscience 96 (3) (2000) 575–583. [PubMed: 10717437]

[56]. Kuljis RO, et al., Degeneration of neurons, synapses, and neuropil and glial activation in a murine Atm knockout model of ataxia-telangiectasia, Proc. Natl. Acad. Sci. U. S. A. 94 (23) (1997) 12688–12693. [PubMed: 9356511]

[57]. Kamsler A, et al., Increased oxidative stress in ataxia telangiectasia evidenced by alterations in redox state of brains from Atm-deficient mice, Cancer Res. 61 (5) (2001) 1849–1854. [PubMed: 11280737]

[58]. Chen P, et al., Oxidative stress is responsible for deficient survival and dendritogenesis in purkinje neurons from ataxia-telangiectasia mutated mutant mice, J. Neurosci. 23 (36) (2003) 11453–11460. [PubMed: 14673010]

[59]. Quick KL, Dugan LL, Superoxide stress identifies neurons at risk in a model of ataxia-telangiectasia, Ann. Neurol. 49 (5) (2001) 627–635. [PubMed: 11357953]

[60]. Gueven N, et al., Dramatic extension of tumor latency and correction of neurobehavioral phenotype in Atm-mutant mice with a nitroxide antioxidant, Free Radic. Biol. Med. 41 (6) (2006) 992–1000. [PubMed: 16934683]

[61]. Stern N, et al., Accumulation of DNA damage and reduced levels of nicotine adenine dinucleotide in the brains of Atm-deficient mice, J. Biol. Chem. 277 (1) (2002) 602–608. [PubMed: 11679583]

[62]. Li J, et al., Cytoplasmic ATM in neurons modulates synaptic function, Curr. Biol. 19 (24) (2009) 2091–2096. [PubMed: 19962314]

[63]. Barlow C, et al., ATM is a cytoplasmic protein in mouse brain required to prevent lysosomal accumulation, Proc. Natl. Acad. Sci. U. S. A. 97 (2) (2000) 871–876. [PubMed: 10639172]

[64]. Li J, et al., Nuclear accumulation of HDAC4 in ATM deficiency promotes neurodegeneration in ataxia telangiectasia, Nat. Med. 18 (5) (2012) 783–790. [PubMed: 22466704]

[65]. Dar I, et al., Investigation of the functional link between ATM and NBS1 in the DNA damage response in the mouse cerebellum, J. Biol. Chem. 286 (17) (2011) 15361–15376. [PubMed: 21300797]

[66]. Levine-Small N, et al., Reduced synchronization persistence in neural networks derived from atm-deficient mice, Front. Neurosci. 5 (2011) 46. [PubMed: 21519382]

[67]. Eilam R, et al., Selective loss of dopaminergic nigro-striatal neurons in brains of Atm-deficient mice, Proc. Natl. Acad. Sci. U. S. A. 95 (21) (1998) 12653–12656. [PubMed: 9770541]

[68]. Eilam R, et al., Late degeneration of nigro-striatal neurons in ATM-/- mice, Neuroscience 121 (1) (2003) 83–98. [PubMed: 12946702]

[69]. Jiang D, et al., Alteration in 5-hydroxymethylcytosine-mediated epigenetic regulation leads to Purkinje cell vulnerability in ATM deficiency, Brain 138 (Pt 12) (2015) 3520–3536. [PubMed: 26510954]

[70]. Campbell A, et al., Mutation of ataxia-telangiectasia mutated is associated with dysfunctional glutathione homeostasis in cerebellar astroglia, Glia 64 (2) (2016) 227–239. [PubMed: 26469940]

[71]. Yamamoto K, et al., Kinase-dead ATM protein causes genomic instability and early embryonic lethality in mice, J. Cell Biol. 198 (3) (2012) 305–313. [PubMed: 22869596]

[72]. Daniel JA, et al., Loss of ATM kinase activity leads to embryonic lethality in mice, J. Cell Biol. 198 (3) (2012) 295–304. [PubMed: 22869595]

[73]. Yamamoto K, et al., Kinase-dead ATM protein is highly oncogenic and can be preferentially targeted by topo-isomerase I inhibitors, Elife 5 (2016).

[74]. Shiloh Y, Ziv Y, The ATM protein: the importance of being active, J. Cell Biol. 198 (3) (2012) 273–275. [PubMed: 22869592]

[75]. Zha S, et al., Complementary functions of ATM and H2AX in development and suppression of genomic instability, Proc. Natl. Acad. Sci. U. S. A. 105 (27) (2008) 9302–9306. [PubMed: 18599436]

[76]. Callen E, et al., Essential role for DNA-PKcs in DNA double-strand break repair and apoptosis in ATM-deficient lymphocytes, Mol. Cell 34 (3) (2009) 285–297. [PubMed: 19450527]

[77]. Dubois NC, et al., Nestin-Cre transgenic mouse line Nes-Cre1 mediates highly efficient Cre/loxP mediated recombination in the nervous system, kidney, and somite-derived tissues, Genesis 44 (8) (2006) 355–360. [PubMed: 16847871]

[78]. Zhang XM, et al., Highly restricted expression of Cre recombinase in cerebellar Purkinje cells, Genesis 40 (1) (2004) 45–51. [PubMed: 15354293]

[79]. Moyal L, et al., Requirement of ATM-dependent monoubiquitylation of histone H2B for timely repair of DNA double-strand breaks, Mol. Cell 41 (5) (2011) 529–542. [PubMed: 21362549]

[80]. Salton M, et al., Involvement of Matrin 3 and SFPQ/NONO in the DNA damage response, Cell Cycle 9 (8) (2010) 1568–1576. [PubMed: 20421735]

[81]. Tzur-Gilat A, et al., Studying the cerebellar DNA damage response in the tissue culture dish, Mech. Ageing Dev. 134 (10) (2013) 496–505. [PubMed: 23583690]

[82]. Tal E, Shiloh Y, Monitoring the ATM-mediated DNA damage response in the cerebellum using organotypic cultures, Methods Mol. Biol. 1599 (2017) 419–430. [PubMed: 28477136]

[83]. Guyenet SJ, et al., A simple composite phenotype scoring system for evaluating mouse models of cerebellar ataxia, J. Vis. Exp. (39) (2010).

[84]. Harno E, Cottrell EC, White A, Metabolic pitfalls of CNS cre-based technology, Cell Metab. 18 (1) (2013) 21–28. [PubMed: 23823475]

[85]. Ziv Y, et al., Chromatin relaxation in response to DNA double-strand breaks is modulated by a novel ATM- and KAP-1 dependent pathway, Nat. Cell Biol. 8 (8) (2006) 870–876. [PubMed: 16862143]

[86]. Fernandez-Vidal A, Vignard J, Mirey G, Around and beyond 53BP1 nuclear bodies, Int. J. Mol. Sci. 18 (12) (2017).

[87]. Andegeko Y, et al., Nuclear retention of ATM at sites of DNA double strand breaks, J. Biol. Chem. 276 (41) (2001) 38224–38230. [PubMed: 11454856]

[88]. Lukas J, Lukas C, Bartek J, More than just a focus: the chromatin response to DNA damage and its role in genome integrity maintenance, Nat. Cell Biol. 13 (10) (2011) 1161–1169. [PubMed: 21968989]

[89]. Baranes-Bachar K, et al., The ubiquitin E3/E4 ligase UBE4A adjusts protein ubiquitylation and accumulation at sites of DNA damage, facilitating double-strand break repair, Mol. Cell 69 (5) (2018) 866–878 e7. [PubMed: 29499138]

[90]. Kanner S, et al., Astrocytes restore connectivity and synchronization in dysfunctional cerebellar networks, Proc. Natl. Acad. Sci. U. S. A. 115 (31) (2018) 8025–8030. [PubMed: 30012604]

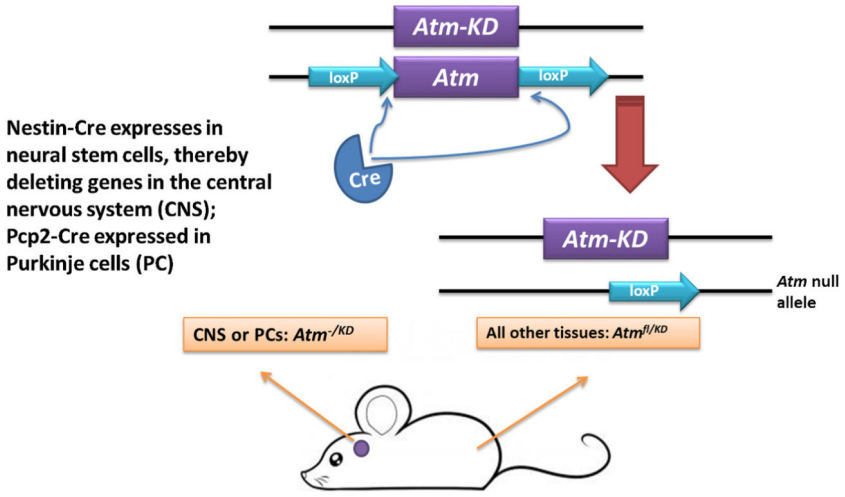

Fig. 1. Generation of mice expressing Atm^{KD} specifically in the central nervous system or in PCs.

Breeding scheme using the Cre-lox system to generate mice expressing kinase-dead Atm in the CNS or specifically in PCs. The animals are compound heterozygotes at the *Atm* locus: one allele is floxed and the other expresses kinase-dead protein (Atm^{KD}). The floxed allele is inactivated by the Cre recombinase, which is expressed in the CNS when driven by the Nestin promoter, or in PCs under the control of the Pcp2 promoter.

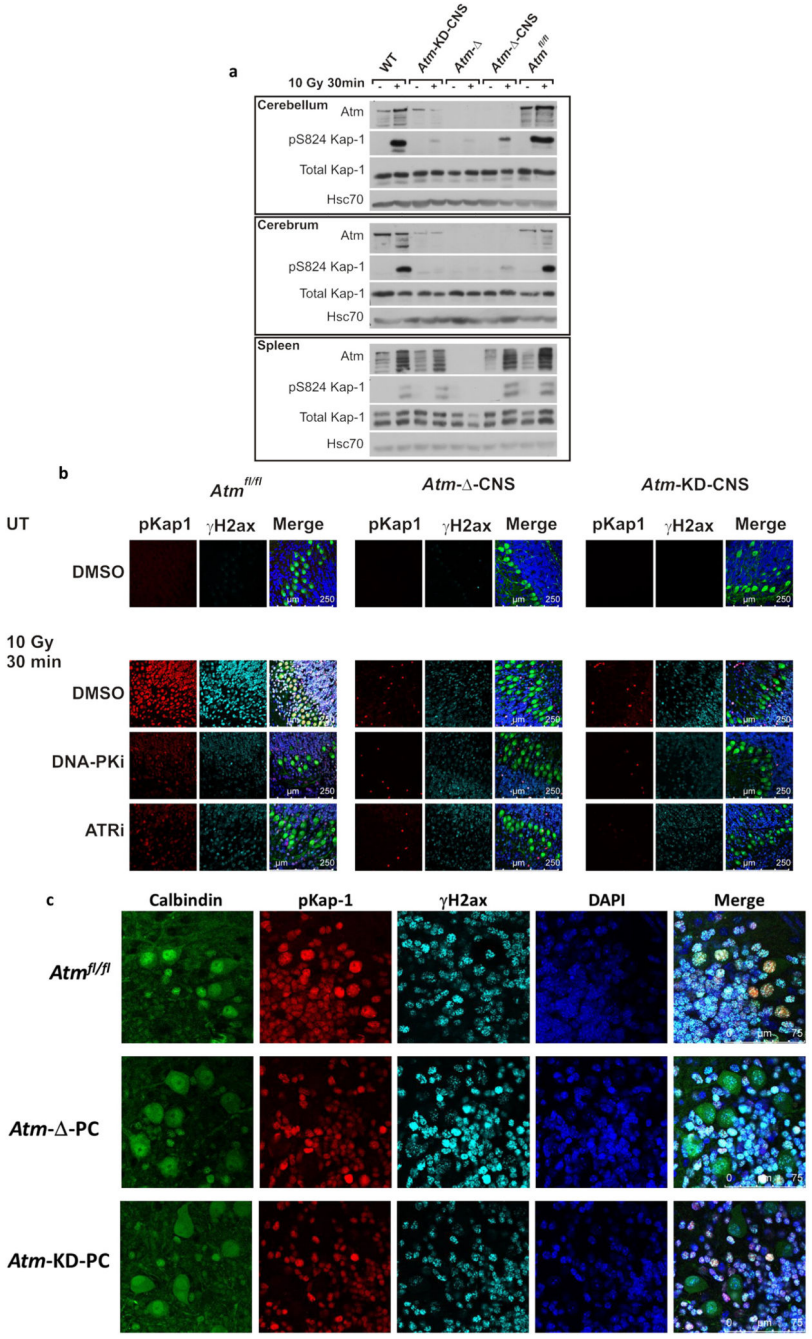

Fig. 2. Atm^{KD} expression in the CNS and functional consequences.

a. Western blotting analysis of cerebellum, cerebrum and spleen with different genotypes after whole-body irradiation with 10 Gy of IR. Phosphorylation of the Atm substrate, Kap-1, 30 min after irradiation was used as a readout of Atm activity in response to DNA damage.

b. Immunostaining of phosphorylated Kap-1 in organotypic cerebellar cultures established from P12 mice. Cultures were pretreated with DMSO or 5 μM NU7441 – a DNA-PK inhibitor (DNA-PKi), or 0.5 μM AZ20 – an ATR inhibitor (ATRi), and irradiated with 10 Gy of IR. The merged images include Calbindin D28k staining (green), which labels PCs and

DAPI staining (blue), which labels cell nuclei. **c.** Similar analysis as in (b) in cerebellar organotypic cultures derived from WT, *Atm*-Δ-PC and *Atm*-KD-PC mice. Note the lack of Kap-1 phosphorylation in PCs only, in both genotypes. PCs are marked by Calbindin D28k staining (green).

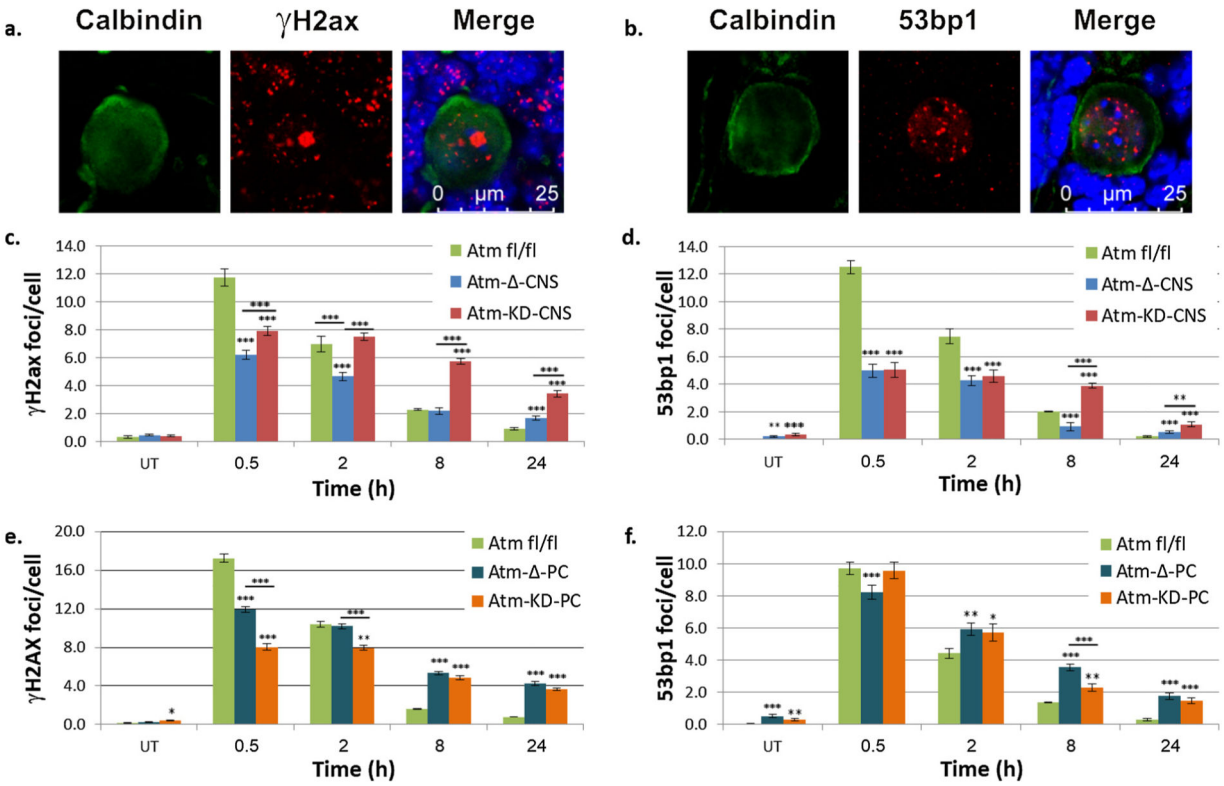

Fig. 3. Atm^{KD} in PCs impairs DSB repair more than Atm absence, in *Atm*-KD-CNS but not in *Atm*-KD-PC mice.

Organotypic cultures were produced from P12 mice and grown for 12 days. **a,b.** Representative images of γH2ax and 53bp1 foci in *Atm*$^{f/f}$ cultures, 30 min after irradiation with 2 Gy of IR. **c,d.** Quantification of γH2ax nuclear foci (c) or 53bp1 foci (d) in PCs from *Atm*-KD-CNS mice. **e,f.** Similar data obtained from *Atm*-KD-PC mice. The results represent the average counts in 90 PCs at each time point in 3 separate experiments. Standard error is as shown. Two-tail *t*-test was used to determine statistical significance between pairs of mice with different genotypes. * $p < 0.05$, ** $p < 0.005$, *** $p < 0.0005$. Non-underlines asterisks refer to the significance of the differences between the *Atm*$^{fl/fl}$ and *Atm*-KO-CNS or *Atm*-KD-CNS genotypes; underlined asterisks refer to the significance of the differences between *Atm*-KO-CNS and *Atm*-KD-CNS.

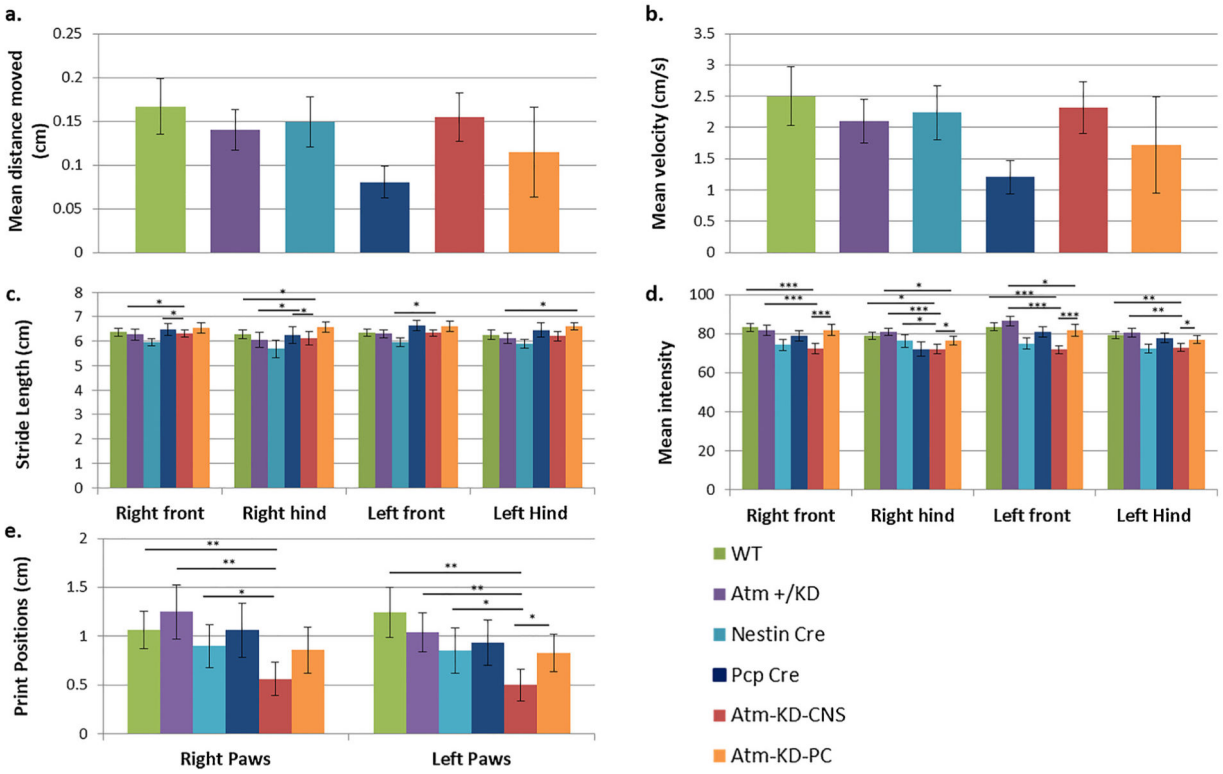

Fig. 4. Expression of Atm^{KD} in the CNS or in PCs does not lead to a discernible behavioral phenotype.

Behavioral tests of 20-month-old mice with different genotypes: *Atm*-KD-CNS (n = 7), *Atm*-KD-PC (n = 9), WT (n = 14), *Atm*$^{+/KD}$ (n = 10), *Nestin-Cre* (n = 8), *Pcp-Cre* (n = 10). General activity of the animals measured using the Open Field test. **a.** Mean distance traveled by the animal over a 20-min period. **b.** Mean velocity of the mouse body center while moving in the arena. **c.** Gait analysis carried out with the CatWalk XT system. The graph depicts stride length – the distance between hind paw subsequent placements. **d.**Mean intensity: mean intensity of the paw pixels forming the maximum area. **e.**Print position: distance between the hind paw position and that of the previously placed front paw on the same body side. Standard errors are shown. Statistical significance was determined using LSD correction for post hoc analysis in ANOVA. * $p < 0.05$, ** $p < 0.005$, *** $p < 0.0005$.

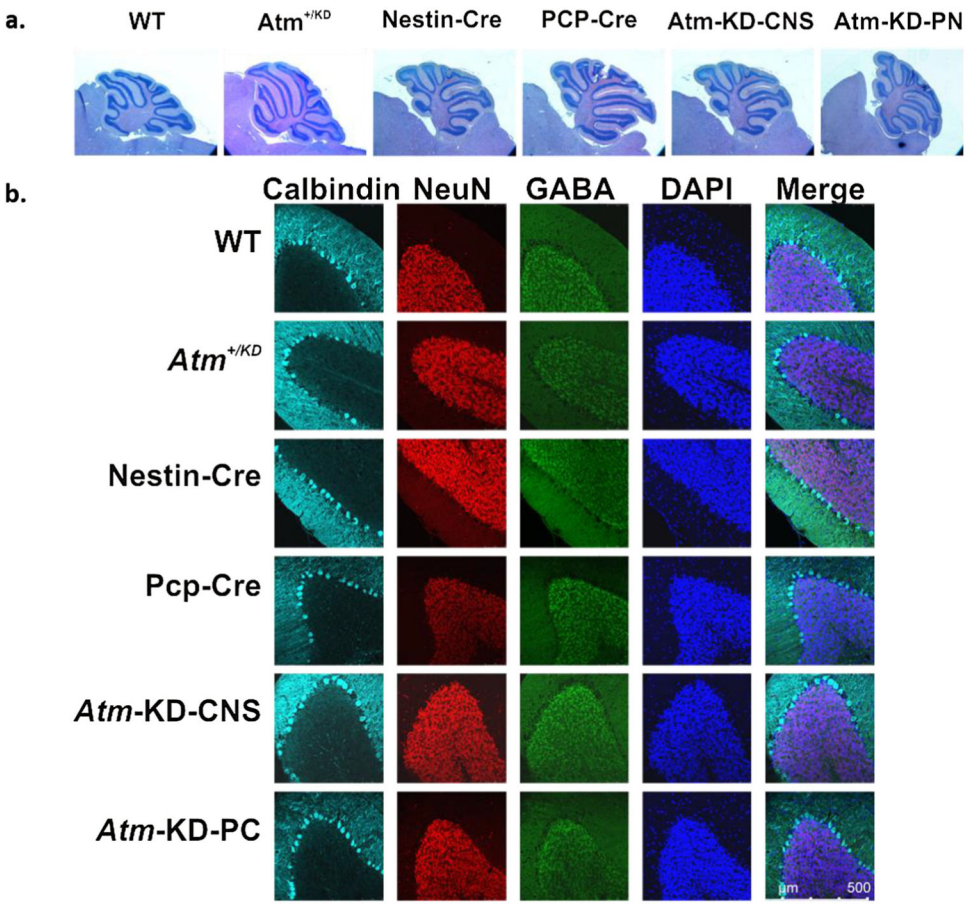

Fig. 5. Normal cerebellar morphology in mice expressing Atm^{KD} in the CNS or in PCs.

Histological analysis of the cerebellum was preformed between ages 1–24 months. Representative images are shown **a.** Hematoxylin-eosin staining of cerebellar paraffin sections produced from 6-month old mice with different genotypes. **b.** Immunostaining of different cell populations in cerebellar sections obtained from 6-month old mice. Calbindin D28k (cyan); NeuN (red) highlighting neurons; GABA (green), which marks GABAergic cells; DAPI (blue).